The Ternary Complex of Cytochrome *f* and Cytochrome *c*: Identification of a Second Binding Site and Competition for Plastocyanin Binding

Peter B. Crowley, Kersten S. Rabe, Jonathan A. R. Worrall, Gerard W. Canters, and Marcellus Ubbink*[a]

The complex of yeast cytochrome c *and cytochrome* f *from the cyanobacterium* Phormidium laminosum *was investigated by NMR spectroscopy. Chemical shift perturbation analysis reveals that residues around the haem edge of cytochrome* c *are involved in the complex interface. Binding curves derived from an NMR spectroscopy titration at 10 mM ionic strength indicate that there are two sites for cytochrome* c *with binding constants of approximately* $2 \times 10^4\,M^{-1}$ *and* $4 \times 10^3\,M^{-1}$*. A protein docking simulation with NMR-derived constraints identifies two sites, at the front (Site I) and back faces (Site II) of the haem region of cytochrome* f*. Site I is homologous to the binding site previously determined for the natural cytochrome* f *partner plastocyanin. Site II may represent the binding site for the Rieske protein in the cytochrome* bf *complex. Cytochrome* c *and plastocyanin are shown to compete for binding at Site I. The competition appears to involve electrostatic screening rather than simple steric occlusion of the binding site.*

KEYWORDS:

cytochromes · electron transport · metalloproteins · NMR spectroscopy · protein docking

Introduction

Interprotein electron transfer (ET) is a key step for many of the processes of cellular metabolism. The formation of transient protein complexes with millisecond lifetimes and μM – mM binding affinities is necessary to maintain high turnover along redox chains.[1] It remains unclear how specificity can be achieved between redox partners under these conditions and, in particular, which elements of the protein structure enable fast ET and are responsible for the control of specificity. Structure determination has accelerated dramatically in recent years. The percentage of crystal structures of redox protein complexes remains however disparately low.[2] Structural characterisation of transient complexes is severely hampered by the difficulty of cocrystallisation. In contrast, NMR spectroscopy methods such as chemical shift perturbation analysis are particularly suited to the study of transient complexes and provide detailed information concerning the complex interface.[3]

In oxygenic photosynthesis, the membrane-bound cytochrome *bf* complex couples proton translocation across the membrane to ET between photosystems II and I, which results in a proton gradient that drives the synthesis of adenosine triphosphate (ATP).[4] The structure of the soluble domain of *Phormidium laminosum* ferrous cytochrome *f* (cyt*f*; Figure 1 A), a component of the *bf* complex, consists of a large and a small domain arranged in an elongated structure of approximately 28.5 kDa.[5–7] The haem-binding motif Cys-X-Y-Cys-His (X and Y denote two different amino acid residues), characteristic of *c*-type cytochromes, occurs near the N-terminus. Unusual features include the sixth ligand Tyr1, which coordinates through the α-amino group, and a chain of five buried water molecules, which extends from behind the haem group to near the protein surface.[8, 9] *P. laminosum* cuprous plastocyanin (Pc; Figure 1 B) is a 10.5 kDa type I copper protein, which functions as the mobile

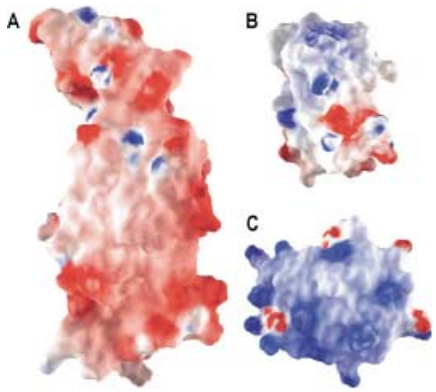

Figure 1. *Electrostatic potential surfaces of (A) cytf,[6] (B) Pc[10] and (C) cytc.[17] Both cytf and cytc are oriented with the haem region facing the viewer.* Pc *is oriented with the copper site at the top. All images were created with a colour ramp for positive (blue) or negative (red) surface potentials with saturation at 10 kT. The potentials were calculated for formal charges only and surfaces were visualised with the GRASP program.[18]*

[a] *Dr. M. Ubbink, P. B. Crowley, K. S. Rabe, Dr. J. A. R. Worrall, Prof. G. W. Canters*
Leiden Institute of Chemistry
Leiden University, Gorlaeus Laboratories
P.O. Box 9502, 2300 RA Leiden (The Netherlands)
Fax: (+31) 71-527-4593
E-mail: m.ubbink@chem.leidenuniv.nl

  1439-4227/02/03/06 $ 20.00+.50/0 ChemBioChem **2002**, 3, 526 – 533

redox partner of cyt*f* and shuttles electrons to photosystem I.[11, 12]

We previously determined the solution structure of the cyt*f*–Pc complex from a plant[13] and a cyanobacterial[14] source by using a novel NMR spectroscopy method based on intermolecular pseudocontact restraints. It was found that a combination of electrostatic and hydrophobic surfaces defines the complex interface between turnip cyt*f* and spinach Pc. In contrast, the complex in *P. laminosum*, a thermophilic cyanobacterium, was found to be predominantly hydrophobic. These differences can be attributed to the different surface charge distributions in the plant and cyanobacterial proteins. In particular, the prominent acidic patches of the plant Pc are completely absent from the cyanobacterial protein,[10] while the hydrophobic patch that surrounds the copper site is more extensive in the latter.[15]

A similar study on the complex of horse cyt*c* and pea Pc revealed that this complex consists of a dynamic ensemble[16] as opposed to the single orientation observed in the cyt*f*–Pc complex. This highlights the importance of studying both physiological and nonphysiological complexes in an effort to deepen our understanding of protein interactions. In this work we have investigated the interaction of yeast ferrous cytochrome *c* (cyt*c*; 12.5 kDa; Figure 1C) with both cyt*f* and Pc from *P. laminosum*. While no complex is formed with Pc, cyt*c* can form a 2:1 complex with cyt*f*. A combination of heteronuclear NMR spectroscopy and protein docking simulations with the BiGGER (bimolecular complex generation with global evaluation and ranking) software[19, 20] was used to determine the orientation of cyt*c* and cyt*f* in the complex. This work provides new insight into the capacity of cyt*f* as a redox partner.

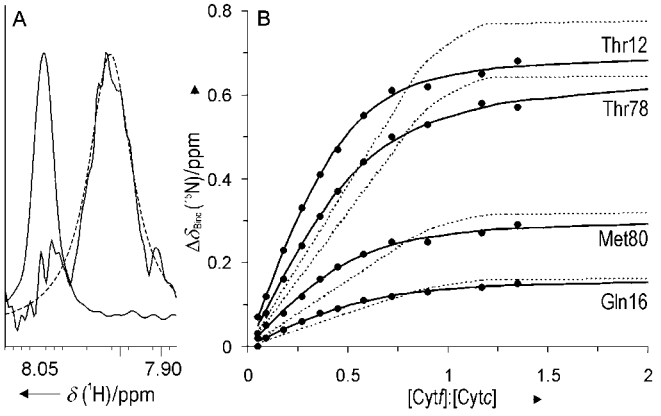

Figure 2. *A) Cross-sections through the $^1H^N$ resonance of the Ala 81 residue in cyt*c *along the F_2 dimension. The peak at 8.05 ppm is the unperturbed resonance in the free protein with a line width at half height of 16 Hz. In the presence of cyt*f *(1.2 equiv), the resonance shifts to 7.96 ppm and the line width at half height increases to 39 Hz. The broken line represents a Lorentzian fit of the resonance in the bound state. B) Titration curves of four amide resonances of cyt*c*. Fits of the curves that assume a 1:1 stoichiometry are shown as dotted lines. The solid lines represent least-squares fits to the model that describes two nonequivalent, noninteracting cyt*c *binding sites per cyt*f*. This model yielded binding constants of approximately $2 \times 10^4\,M^{-1}$ and $4 \times 10^3\,M^{-1}$.*

Results

The complex of cyt*f* and cyt*c*

Comparison of the ^{1}H-^{15}N HSQC spectra of free ^{15}N-cyt*c* and ^{15}N-cyt*c* in the presence of cyt*f* revealed distinct differences arising from complex formation. In the complex, cyt*c* experiences a longer rotational correlation time manifested as a general broadening of the amide resonances. The presence of cyt*f* resulted in approximately 25 Hz broadening of the cyt*c* resonances (Figure 2A). In addition to line broadening effects, chemical shift perturbation ($\Delta\delta_{Bind}$) was observed for a number of resonances (Figure 2A and B). The magnitude of the line broadening was similar for both shifted resonances and resonances which did not shift. This behaviour typifies a fast exchange process on the NMR time scale and yields a single averaged resonance for the bound and free forms of cyt*c*. With the addition of increasing amounts of cyt*f*, the line broadening and chemical shift perturbation of ^{15}N-cyt*c* resonances increased towards a maximum. Within experimental error, identical $\Delta\delta_{Bind}$ effects were observed for the reverse titration in which cyt*c* was titrated into cyt*f*. Titration curves of $\Delta\delta_{Bind}$ values versus the molar ratio of cyt*f*:cyt*c* are plotted in Figure 2B. A fit of the curves that assumes a 1:1 stoichiometry (dotted lines) clearly fails to fit the experimental data. A binding model with two cyt*c* molecules per cyt*f* resulted in a greatly improved fit. The two-site model for nonequivalent, noninteracting sites[21, 22] (solid line) yielded binding constants of approximately $2 \times 10^4\,M^{-1}$ and $4 \times 10^3\,M^{-1}$ (Table 1).

Table 1. *Binding constants and maximum chemical shift changes for complex formation between cyt*f *and cyt*c*.[a]*

Residue	K^a [$10^4\,M^{-1}$]	$\Delta\delta^a_{max}$ [ppm]	K^b [$10^3\,M^{-1}$]	$\Delta\delta^b_{max}$ [ppm]
Gln 16	2.0	0.19	4.2	0.08
Met 80	1.8	0.32	4.3	0.26
Thr 78	2.0	0.74	4.5	0.34
Thr 12	2.0	0.61	4.2	1.00

*[a] Values were derived from a fit of the data in Figure 2 with the model for two nonequivalent, noninteracting sites on cyt*f *(see the Experimental Section for details).*

At equimolar concentrations of ^{15}N-cyt*c* and cyt*f*, twenty-two of the ninety-eight resolved backbone amides demonstrated significant $\Delta\delta_{Bind}$ values, which ranged from -0.12 to 0.07 ppm and from -0.69 to 0.11 ppm for the amide proton ($^1H^N$) and nitrogen (^{15}N) nuclei, respectively. These chemical shift changes identify the region of cyt*c* involved in the complex interface with cyt*f*. Figure 3A shows the location of the affected residues in the crystal structure of cyt*c*,[17] with each residue coloured according to its largest $\Delta\delta_{Bind}$ value. The affected amides cluster around the exposed edge of the haem group on the front face of the protein. Residues Thr 12, Thr 78 and Lys 79 experience the largest effects.

The ferrous form of cytochrome *c* gives rise to several resonances in the upfield region of the 1D ^{1}H NMR spectrum. These resonances have been assigned to the side-chain protons

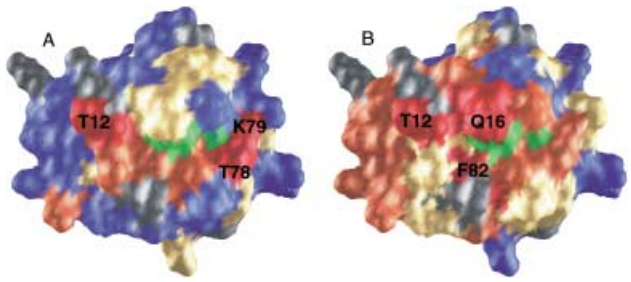

Figure 3. *Chemical shift maps of cytc in the presence of (A) cytf and (B) cytochrome c peroxidase (Ccp).[32] Residues are coloured according to the chemical shift perturbation they experience (ppm): blue, < 0.03 (^{1}H), ≤ 0.1 (^{15}N); cream, ≤ 0.06 (^{1}H), ≤ 0.3 (^{15}N); orange, ≤ 0.10 (^{1}H), ≤ 0.6 (^{15}N); red, ≤ 1.0 (^{1}H), ≤ 2.0 (^{15}N). Prolines and unassigned residues are indicated in grey. The haem group is coloured green.*

of the sixth haem ligand,[23, 24] residue Met 80 in the case of yeast cytc.[25] In agreement with the heteronuclear data for Met 80, small chemical shift changes were observed for these upfield peaks in the presence of cyt*f* (Table 2). Four resonances were observed in the upfield region of the ^{1}H NMR spectrum of ferrous cyt*f*, which disappear in the ferric form (Figure 4). Two of these resonances have been reported before in an earlier NMR spectroscopy study on plant cyt*f*.[26] The exceptionally large upfield shifts imply that the signals arise from protons in the vicinity of the haem group, probably from the ligand Tyr 1. These

Table 2. *Chemical shifts of the upfield resonances in the 1D ^{1}H NMR spectra of free cytc, free cytf and a sample of the cytf/cytc (0.9:1.0) complex.*

Free Protein [ppm]	Complex [ppm]	$\Delta\delta_{Bind}$ [ppm]
cytc M80		
β −0.17	−0.19	−0.02
β −2.40	overlap[a]	–
γ −1.72	−1.77	−0.05
γ −3.68	−3.73	−0.05
ε −3.14	−3.2	−0.06
cytf		
−2.47	overlap[a]	–
−3.33	−3.28	0.05
−6.69	−6.66	0.03
−7.87	−7.85	0.02

[a] In the spectrum of the sample containing cytc and cyt*f* the −2.4 ppm resonances of the two proteins overlap.

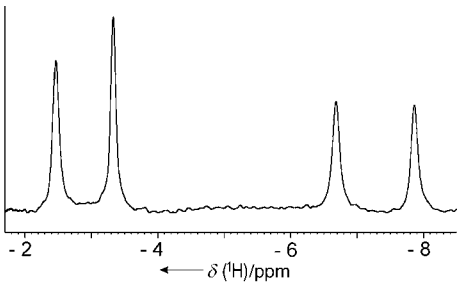

Figure 4. *The upfield resonances of ferrous cytf as observed in the 1D ^{1}H NMR spectrum.*

resonances experience chemical shift perturbation in the presence of cytc (Table 1), which indicates that at least one of the binding sites for cytc is located near the haem group of cyt*f*.

To investigate ionic strength effects on the complex, ^{1}H-^{15}N HSQC spectra were acquired on a cyt*f*/cyt*c* (1.4:1) sample, over a range of NaCl concentrations (0 – 200 mM). Both the line broadening and the $\Delta\delta_{Bind}$ values were dependent on the NaCl concentration. The observed chemical shift perturbation of the twenty-two affected amides is plotted as a function of the salt concentration in Figure 5. The chemical shift perturbation of free

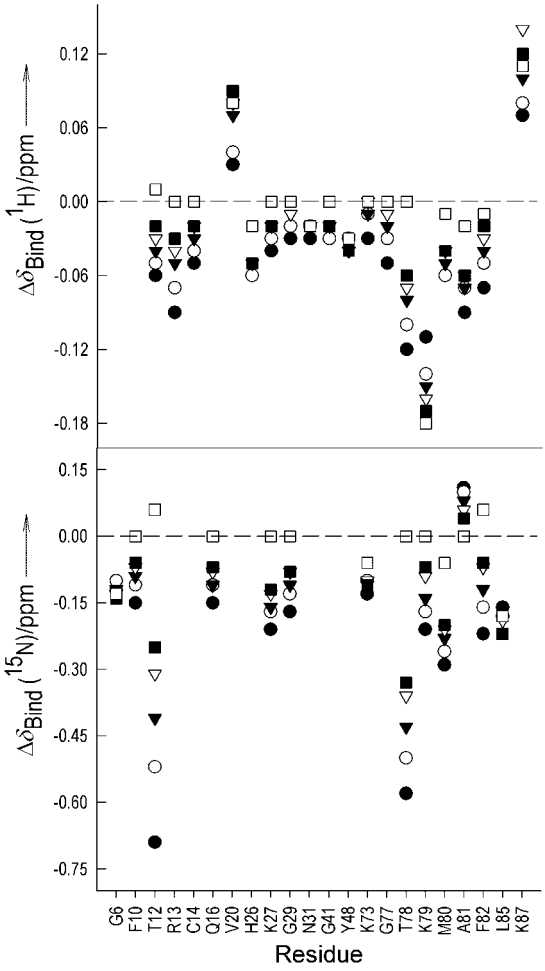

Figure 5. *Salt dependence of $\Delta\delta_{Bind}$ values for all twenty-three affected backbone amide resonances observed in the complex of cytc and cytf at (●) 0 mM NaCl, (○) 50 mM NaCl, (▼) 100 mM NaCl, (▽) 150 mM NaCl and (■) 200 mM NaCl. (□) represents the chemical shift perturbation of free cytc resonances caused by the presence of 200 mM NaCl.*

cytc resonances due to the presence of 200 mM salt is represented by open squares in the plot. At 200 mM NaCl the magnitude of the $\Delta\delta_{Bind}$ values decreased by sixty percent on average, which indicates a strong electrostatic contribution to complex formation. The line broadening effects also decreased proportionally. Similar results were obtained for a cytc/cyt*f* (2:1) sample. The $\Delta\delta_{Bind}$ value for the salt-sensitive resonances of residues Val 20, Lys 79 and Lys 87, do not decrease towards zero but rather towards the value for free cytc at high salt.

Protein Docking

To obtain intermolecular pseudocontact shifts for structure determination it is necessary to subtract the appropriate diamagnetic control from measurements on a complex in which at least one of the species is paramagnetic. In the cyt*f* – cyt*c* complex it is only possible to measure the fully oxidised or fully reduced samples, which complicates the possibility of obtaining reliable data. As an alternative to the use of pseudocontact shifts, a docking simulation between cyt*f* and cyt*c* was performed by using the BiGGER software.[19, 20] 5000 putative geometries generated by BiGGER were independently assessed and ranked in terms of both the standard scoring function[19] and the experimentally obtained data. The results of each ranking procedure are presented in Figure 6. The results that used only the scoring function as implemented by the BiGGER program were clear cut (Figure 6 A). The front face of the haem region in cyt*f* (Site I) is unequivocally identified as the binding site for cyt*c*. When experimental constraints were used to rank the docking configurations, however, the results were significantly different (Figure 6 B). While Site I remains the favoured site of interaction, several other regions of the cyt*f* surface were identified as potential binding sites for cyt*c*. In particular, there is a preponderance of favourable docking orientations directly opposite Site I. Binding curves derived from the NMR spectroscopy titration indicate that there are two binding sites for cyt*c*.

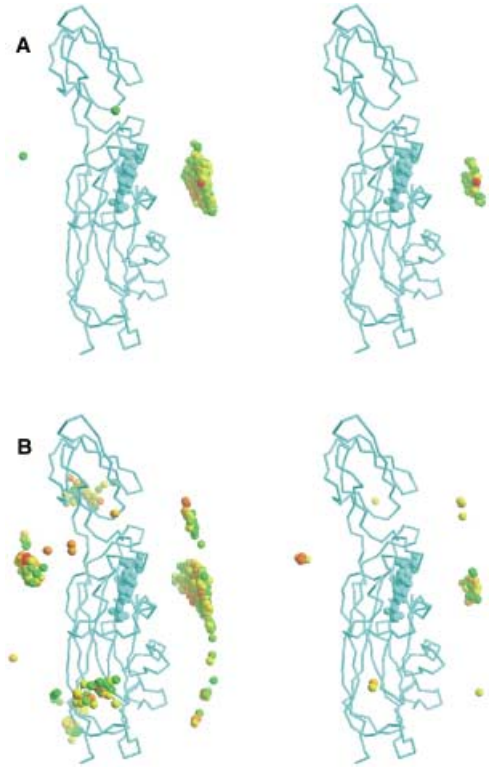

Figure 6. *Comparison of (A) the ab initio and (B) the experimentally ranked docking geometries as generated by the BiGGER program.[19] Cyt*f *is depicted as the C^{α} trace with the haem group in spacefill. The geometric centre of cyt*c *is represented by spheres in each of one thousand docking geometries (left) and the top fifty geometries (right). The colour coding indicates the ranking position on a scale from green to red with red to indicate more favourable ranking.*

The experimentally ranked docking calculations suggest that these binding sites are Site I and Site II. These two top-ranking docking configurations are illustrated in Figure 7. Cyt*f* is sandwiched between two molecules of cyt*c*, which are approximately interchangeable by a 180° rotation about an axis defined by the Fe atoms of each cyt*c* and centred on the C^{α} atom of the G 158 residue in cyt*f*. The Fe – Fe distances between cyt*f* and cyt*c* are 14.1 Å at Site I and 19.0 Å at Site II. Of the thirty-one constraints used in the experimental ranking procedure, eight were violated at Site I, and nine were violated at Site II.

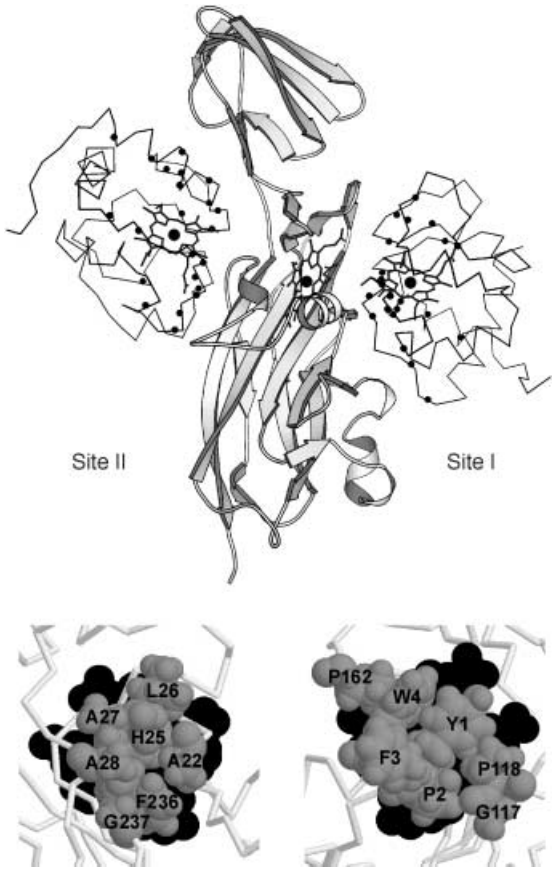

Figure 7. *The top-ranking orientations of cyt*c *at Site I and Site II. Cyt*f *is depicted in ribbon representation and cyt*c *as the C^{α} trace with the residues for which constraints were used indicated by black spheres for the backbone N atom. The two binding sites on cyt*f *are also shown in detail. Aliphatic and aromatic residues are coloured grey and the haem group is coloured black. The figure was drawn with the program Molscript.[27]*

Cyt*c* and Pc

No significant effects were observed in the ^{1}H-^{15}N HSQC spectra upon titration of *P. laminosum* Pc into yeast ^{15}N-cyt*c*. Despite the addition of 2.5 molar equivalents of Pc, the cyt*c* resonances did not demonstrate any line broadening and only one backbone amide experienced a change in chemical shift. The resonance of the amide proton, $^{1}H^{N}$, of Lys 79 was shifted by 0.05 ppm. Assignments for cyt*c* at 200 mM NaCl indicate that this $^{1}H^{N}$ proton, whose signal shifts by almost 0.2 ppm, has one of the most salt-sensitive resonances in the protein (Figure 5). It is likely

that the small shift of this proton in the presence of Pc reflects a change in the solvent ionic strength, which possibly arises from electrostatic screening by Pc. In contrast to the results reported for the interactions of cyt*c* and cyt*f*, it can be concluded that no complex is formed between cyt*c* and Pc. This is in agreement with laser flash photolysis measurements on horse heart cyt*c* and Pc, which demonstrate that there is no significant electron transfer reaction (C. Lowe, M. A. De la Rosa; personal communication).

Competition for the binding site on cyt*f*

Site I of cyt*f* has been identified as a binding site for both cyt*c* (this work) and the natural partner Pc.[14] For this reason, we investigated competition between *P. laminosum* Pc and cyt*c* for Site I on cyt*f*. Complex formation in a cyt*f*/^{15}N-cyt*c* (1:1) sample was monitored as described above. Unlabelled Pc was titrated into this sample to 1.6 molar equivalents and competition for binding at Site I was inferred from changes in the $\Delta\delta_{Bind}$ effects observed for the ^{15}N-labelled cyt*c*. A similar experiment was performed with a 1:1 sample of cyt*f* and ^{15}N-Pc. Unlabelled cyt*c* was titrated into this sample to 2.0 molar equivalents. Regions from the overlaid ^{1}H-^{15}N HSQC spectra of the free proteins, the complex and the complex in the presence of the "competitor" protein are illustrated in Figure 8. The $\Delta\delta_{Bind}$ value decreased as the concentration of competitor was increased. Likewise, the magnitude of the line broadening decreased, which indicates that more of the labelled protein was in the free form. It can therefore be concluded that the addition of competitor protein tends to disrupt the observed complex. The results of the competition experiments are plotted in Figure 9. $\Delta\delta_{Bind}$ values observed for ^{15}N-cyt*c* resonances decreased on average by fifty percent in the presence of 1.6 equivalents of *P. laminosum* Pc. For some resonances there was no significant decrease. Anomalous effects were observed for Lys 79 and Lys 87, which showed behaviour similar to that observed in the salt titration (Figure 5).

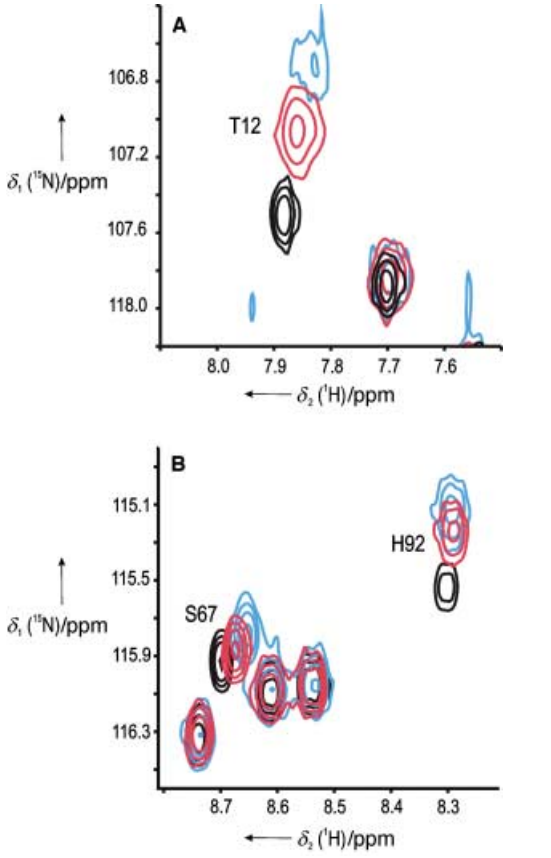

Figure 8. *A) A region of the overlaid ^{1}H-^{15}N HSQC spectra of free ^{15}N-cyt*c *(black), a 1:1 complex of cyt*c *and cyt*f *(blue) and a 1:1 cyt*c*/cyt*f *solution with 1.6 M equiv Pc (red). B) A region of the overlaid ^{1}H-^{15}N HSQC spectra of free ^{15}N-Pc (black), a 1:1 complex of Pc and cyt*f *(blue) and a 1:1 Pc/cyt*f *solution with 2.0 M equiv cyt*c *(red).*

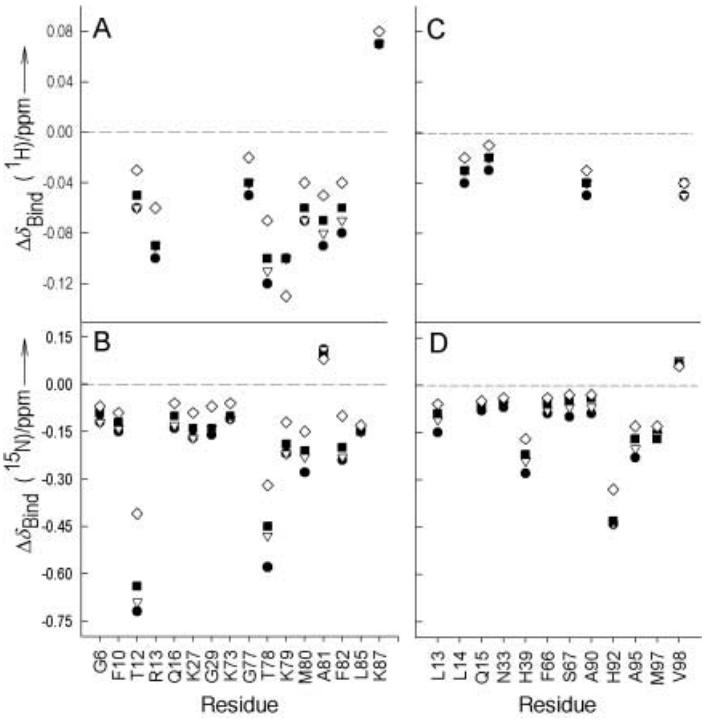

Figure 9. *(A) and (B) illustrate the effect of the presence of (●) no Pc, (▽) 0.5 equiv, (■) 1 equiv and (◇) 1.6 equiv Pc on $\Delta\delta_{Bind}$ values for a 1:1 ^{15}N-cyt*c*/cyt*f *mixture. (C) and (D) illustrate the effect of the presence of (●) no cyt*c*, (▽) 0.5 equiv, (■) 1 equiv and (◇) 2.0 equiv cyt*c *on $\Delta\delta_{Bind}$ values for a 1:1 ^{15}N-Pc/cyt*f *mixture.*

Similar results were seen for the case in which the effects on bound ^{15}N-Pc were observed. At two equivalents of cyt*c*, the $\Delta\delta_{Bind}$ values observed for ^{15}N-Pc resonances decreased by 60%. It has previously been shown that the complex between cyt*f* and Pc remains intact in the presence of 200 mM NaCl.[14] In contrast, the cyt*f* – cyt*c* complex is disrupted at high ionic strength. A sample containing cyt*c*/cyt*f*/^{15}N-Pc (2:1:1) was also investigated at 200 mM NaCl. As might be expected, several of the ^{15}N-Pc resonances were restored to their original $\Delta\delta_{Bind}$ values as observed in the absence of cyt*c*. However most of the resonances were unaffected.

Discussion

Interactions of cyt*f* and cyt*c*

Although cyt*c* is a nonphysiological partner for cyt*f*, the results presented above demonstrate that the proteins are capable of

complex formation. Considering the net charges under neutral pH conditions (−14 for cyt*f* and +8 for cyt*c*), a strong electrostatic attraction is expected for these partners. Addition of NaCl to increase the ionic strength tends to inhibit the interaction of the proteins, which indicates that the complex is indeed electrostatic in nature. These results are in agreement with the work of Wagner et al., who have shown that the rate of reduction of horse cyt*c* by intact cytochrome *bf* molecules from *P. laminosum* decreased sharply above an ionic strength of 70 mM.[28] Pc has a net charge of −3 and does not form a complex with yeast cyt*c*. In a previous ^{1}H NMR spectroscopy study, small chemical shift changes (< 0.05 ppm) were observed for horse cyt*c* in the presence of pea plastocyanin.[16] These results were interpreted as representing a dynamic ensemble of electrostatic complexes. In this case the acidic patches of the plant Pc favour an electrostatic interaction.

A model for specific complex formation based on electrostatics alone is, however, clearly inadequate. It has been shown that hydrophobic interactions play a vital role in stabilising protein complexes.[29] In order to obtain a specific complex from a dynamic ensemble it is necessary to bury hydrophobic residues in the complex interface. The relatively large chemical shift changes observed in the presence of cyt*f* suggests that cyt*c* maintains a specific orientation for a significant fraction of the complex lifetime. A combination of NMR spectroscopy and protein docking simulations made it possible to identify two cyt*c* binding sites on cyt*f*. This is in stark contrast to both the dynamic ensemble observed for cyt*c* with plant Pc,[16] and to the absence of complex formation with the cyanobacterial Pc.

When cyt*c* binds at Site I of cyt*f*, the hydrophobic residues around the two haem groups are brought into close proximity. A similar hydrophobic stabilisation can be envisaged when cyt*c* is bound at Site II. In this orientation the complex interface encompasses a cluster of six hydrophobic residues surrounding the carbonyl oxygen of residue His 25 and the fifth haem ligand of cyt*f* (Figure 7). Four of these residues (Ala 22, Leu 26, Phe 236 and Gly 237) are invariant across the thirty-three known cyt*f* sequences. The Ala 27 residue, which participates in the buried water chain, is conserved in all but two sequences. The amino acid Ala 28 is strongly conserved among cyanobacterial sequences but occurs predominantly as a Gln or Asn residue in plant and algal sequences. It is noteworthy that residues Phe 236 and Gly 237 occur in the sequence Gly-Gly-Phe-Gly-Gln, the only invariant element of the primary structure of cyt*f* apart from the haem-binding motif. The sequence alignment indicates that Site II is a highly conserved region of cyt*f*. Furthermore the site is hydrophobic in nature. In general, redox proteins are characterised by a hydrophobic patch that surrounds the port of entry and exit for electrons. This suggests that Site II may be a true electron transfer site, possibly for the Rieske protein in the cytochrome b*f* complex. A crystal structure is available for the C-terminal domain of the Rieske protein from spinach.[30] Docking simulations between this fragment and cyt*f* resulted in favourable docking at both Site I and site II. In the absence of a crystal structure of the cytochrome *bf* complex, the accessibility of Sites I and II of cyt*f* in vivo remains to be established. It has been suggested that cyt*f* lies close to the membrane within the tight confines of the thylakoid space.[31]

A clearly defined region on the surface of cyt*c* is involved in the interaction with cyt*f* (Figure 3 A). The complex of yeast cyt*c* and its physiological partner cytochrome *c* peroxidase was characterised recently by heteronuclear NMR spectroscopy.[32] Figure 3 B illustrates the chemical shift map of cyt*c* in the presence of C*c*p. The gross features of the binding site on cyt*c* are similar for the complexes with both cyt*f* and C*c*p, although the interface is considerably more extensive in the latter. On average, larger $\Delta\delta_{Bind}$ effects were observed for the C*c*p complex, which was investigated at 100 mM NaCl. These differences can be attributed to co-evolution of cyt*c* and C*c*p to optimise molecular recognition and complementarity, which gives rise to a binding constant at least one order of magnitude higher than the nonphysiological complex.

The structure of the *P. laminosum* Pc – cyt*f* complex was determined recently by using pseudocontact restraints.[14] It was found that hydrophobic interactions predominate in this complex. In contrast, the nonphysiological cyt*c* – cyt*f* complex also relies on favourable electrostatic attractions between the proteins. It is clear, therefore, that cyt*f* can utilise different interactions with different partners in vitro. The behaviour in vivo is more complicated as was demonstrated for the oxidation of cyt*f* in *Chlamydomonas reinhardtii*. While electrostatics are important for the in vitro reaction with Pc, it was demonstrated that the removal of complementary charges on cyt*f* had no effect on the reaction in whole cells.[33]

Competition for the Pc binding site

The present work demonstrates that cyt*f* has two binding sites for cyt*c*, one of which (Site I) is homologous to the Pc binding site. It has also been shown that cyt*c* and *P. laminosum* Pc do not form a complex. Therefore it was possible to investigate competition between Pc and cyt*c* for Site I on cyt*f*. It is clear from Figures 8 and 9 that the presence of the competitor protein prevents complex formation between cyt*f* and the labelled protein (cyt*c* or Pc). The results appear to be similar in both cases. However, cyt*c* is the stronger competitor since it can bind at two sites on cyt*f*. The binding constant for the Pc – cyt*f* complex is on the order of $10^2\,M^{-1}$. It is surprising therefore that Pc is capable of competing with cyt*c*. This suggests that the mode of competition is more complicated than mere steric occlusion of the binding site.

It was noted that the resonances of residues Lys 73 and Lys 87 behaved similarly in both the salt titration (Figure 5) and the competition experiments (Figure 9). It is conceivable therefore, that the inhibition of cyt*c* binding in the presence of Pc could be the result of electrostatic screening. In this case, Pc behaves as a counterion to cyt*c* and thereby hinders the interaction with cyt*f*. This idea is supported by the observation that the Lys 79 residue of cyt*c* is similarly sensitive to the presence of either Pc or NaCl, as described above. Furthermore the bimolecular association step is different for a molecule approaching free cyt*f* from that for a molecule approaching cyt*f* in a complex with either partner. Thus, while electrostatic effects are not crucial for the cyt*f* – Pc

complex, they may gain in importance when a molecule of cytc is already bound to cytf and the net effective charge is -6 (or $+2$ for two molecules of bound cytc) rather than -14. This change in charge could lead to an enhancement of the bimolecular association. Additional complications concern the possibility of fluxionality. When one site is already occupied the second protein may bind at an alternative site with increased affinity.[34] Clearly these questions need to be addressed in the future with the hope of understanding the specificity and dynamics of proteins with multifarious roles in the cell.

The identification of two cytc binding sites may be of relevance for the interactions of cytf with the natural partner cytochrome c_6, which functions as an alternative electron carrier to Pc in certain cyanobacteria and algae when grown under copper-depleted conditions.[35, 36] The complex of cytf and cytochrome c_6 is currently under investigation.

Experimental Section

Protein preparation: All protein samples were produced by heterologous expression in *E. coli*. Unlabelled and uniformly ^{15}N-labelled cytc (C102T) were isolated and purified as described previously.[37, 38] The preparation of unlabelled cytf and Pc and uniformly ^{15}N-labelled Pc was performed according to previously published methods.[14, 39]

NMR spectroscopy samples: Protein interactions were investigated for the diamagnetic species only and reducing conditions were maintained by the presence of sodium ascorbate. Protein solutions were concentrated to the required volume in Millipore Ultrafree centrifuge tubes with a 5 kDa molecular weight cut-off and exchanged into a solution containing potassium phosphate (10 mM; pH 6.0), D_2O (10%) and sodium ascorbate (1.0 mM). Protein concentrations were determined by optical spectroscopy by using extinction coefficients $\varepsilon_{550} = 27.5\ \mathrm{mM^{-1}\,cm^{-1}}$ and $\varepsilon_{556} = 31.5\ \mathrm{mM^{-1}\,cm^{-1}}$ for the ferrous forms of cytc and cytf, respectively. The concentration of Pc was determined for the cupric form by using an ε_{597} value of $4.3\ \mathrm{mM^{-1}\,cm^{-1}}$.

To investigate complex formation between cytc and cytf, microlitre aliquots of a 4.2 mM cytf stock solution were titrated into an NMR spectroscopy sample containing ^{15}N-cytc (0.85 mM). After each addition of protein, the pH value of the sample was verified and ^{1}H-^{15}N HSQC spectra were recorded. Reverse titrations were also performed in which ^{15}N-cytc (1.5 mM) was titrated into cytf samples (0.4 and 0.7 mM). To study the effects of ionic strength on the complex, a sample containing cytf/cytc (1.4:1) was titrated with NaCl to a final concentration of 200 mM. A similar salt titration was performed on a 2:1 cytc/cytf sample. To study the interactions of cytc and Pc, the latter protein was titrated into a ^{15}N-cytc sample (0.25 mM) to 2.5 molar equivalents. Competition between cytc and Pc for the binding site on cytf was investigated by using ternary mixtures. Samples containing cytf (0.4 mM) and the labelled partner, ^{15}N-Pc or ^{15}N-cytc (0.4 mM), were prepared. Microlitre aliquots of the third component, unlabelled Pc or unlabelled cytc, were titrated to approximately 0.5, 1 and 2 molar equivalents and the effects on the labelled protein were observed. Control measurements were recorded on the pure proteins under identical conditions.

NMR spectroscopy: All measurements were performed on a Bruker DMX 600 NMR spectrometer at 300 K. ^{1}H-^{15}N HSQC[40] spectra were acquired with spectral widths of 40.0 ppm (^{15}N) and 13.9 ppm (^{1}H) to investigate the interactions of cytc with cytf. Spectra of the ternary mixtures were acquired with the same spectral widths except for those containing ^{15}N-Pc, which were acquired with spectral widths of 40.0 ppm (^{15}N) and 17.9 ppm (^{1}H). The XWINNMR program was used for spectral processing, and analysis of the chemical shift perturbation with respect to the free protein was performed with the XEASY software.[41] Nuclei that experience chemical shift perturbation as a result of binding ($\Delta\delta_{\mathrm{Bind}}$) were identified by subtraction of the assignments for the free protein from the assignments in the complex, as shown in Equation (1).

$$\Delta\delta^{i}_{\mathrm{Bind}} = \delta^{i}_{\mathrm{complex}} - \delta^{i}_{\mathrm{free}} \tag{1}$$

$\delta^{i}_{\mathrm{complex}}$ and $\delta^{i}_{\mathrm{free}}$ are the chemical shifts experienced by nucleus i in the complex and in the free protein, respectively.

Binding curves: Binding curves were obtained by plotting $\Delta\delta_{\mathrm{Bind}}$ values against the molar ratio of cytf:cytc. The data were fitted to either a one-site or a two-site model by using the program SCIENTIST (MicroMath, Salt Lake City, UT). The NMR spectroscopy experiment cannot explicitly distinguish binding at Site I from binding at Site II. Therefore, to avoid confusion, the model is described in general terms for site a and site b. In the case of cytc binding to two distinct sites on cytf, $\Delta\delta_{\mathrm{Bind}}$ is the sum of the contributions from each site as given by Equation (2).

$$\Delta\delta_{\mathrm{Bind}} = \Delta\delta^{\mathrm{a}}_{\mathrm{max}}\frac{fc^{\mathrm{a}}}{c_{\mathrm{t}}} + \Delta\delta^{\mathrm{b}}_{\mathrm{max}}\frac{fc^{\mathrm{b}}}{c_{\mathrm{t}}} \tag{2}$$

$\Delta\delta^{\mathrm{a}}_{\mathrm{max}}$ and $\Delta\delta^{\mathrm{b}}_{\mathrm{max}}$ are the maximum chemical shift changes at site a and site b, respectively, fc^{a} and fc^{b} represent the amount of cytc bound at site a and site b on cytf and c_{t} is the total amount of cytc. The binding constant for site a is given by Equation (3),

$$K^{\mathrm{a}} = \frac{fc^{\mathrm{a}}}{cf} \tag{3}$$

where c and f are the concentrations of free cytc and free cytf. Assuming nonequivalent, noninteracting binding sites, Equation (3) can be rewritten as Equation (4).

$$K^{\mathrm{a}} = \frac{fc^{\mathrm{a}}}{(c_{\mathrm{t}} - fc^{\mathrm{a}} - fc^{\mathrm{b}})\,(f_{\mathrm{t}} - fc^{\mathrm{a}})} \tag{4}$$

By analogy, a similar equation can be derived for K^{b} and combination with Equation (4) yields the relationships given by Equations (5) and (6).

$$fc^{\mathrm{a}} = K^{\mathrm{a}}(c_{\mathrm{t}} - fc^{\mathrm{a}} - fc^{\mathrm{b}})(f_{\mathrm{t}} - fc^{\mathrm{b}}) \tag{5}$$

$$fc^{\mathrm{a}} = c_{\mathrm{t}} - fc^{\mathrm{b}} - \frac{fc^{\mathrm{b}}}{K^{\mathrm{b}}(f_{\mathrm{t}} - fc^{\mathrm{b}})} \tag{6}$$

f_{t} and c_{t} are related to the concentration of the stock solution of cytf (f_0), the initial concentration of cytc (c_0) and the molar ratio R ($f_{\mathrm{t}}/c_{\mathrm{t}}$) by Equations (7) and (8).

$$f_{\mathrm{t}} = \frac{R f_0 c_0}{(R c_0) + f_0} \tag{7}$$

$$c_{\mathrm{t}} = \frac{f_0 c_0}{(R c_0) + f_0} \tag{8}$$

Numerical solutions to Equation (2) were obtained by nonlinear least squares fitting of the model, with R and $\Delta\delta_{\mathrm{Bind}}$ values as the independent and dependent variables, respectively.

Protein docking: The coordinates for cyt*f*,[6] cyt*c*[17] and the Rieske protein[30] were obtained from the Brookhaven Protein Data Bank (accession codes 1ci3, 1ycc and 1rfs, respectively). Docking simulations between cyt*f* and cyt*c* were performed by using the docking program BiGGER. The procedure implemented by this program has been adequately described in the literature[19, 20] and is presented here in brief. The program consists of two modules. In the first module, a population of docked geometries with maximal surface matching and favourable intermolecular amino acid contacts is generated. To do this, the shape of each molecule is represented by a 3D matrix of 1 Å^3 cells and an exhaustive grid search is performed in which the matrix that defines one molecule systematically explores the matrix that represents the partner molecule. In the second module the docking results are ranked according to a global scoring function composed of four terms; surface matching, side-chain contacts, electrostatics and solvation energy.

The docked geometries were also ranked, independently of the standard method, by using the experimentally obtained information about the complex interface. Nuclei that experienced a $|\Delta\delta_{Bind}| \geq 0.03$ ($^1H^N$) or > 0.10 (^{15}N) were translated into distance constraints on the assumption that they must be within 5 Å of any atom on the partner protein. The scoring is based, therefore, on the number of satisfied constraints in each of the docked geometries. A total of thirty-one NMR-spectroscopy-derived constraints were used in the experimental ranking procedure.

Dr. C. Erkelens is acknowledged for his assistance with the NMR facilities. K.S.R. acknowledges the Socrates/Erasmus program.

[1] D. S. Bendall in *Protein Electron Transfer* (Ed.: D. S. Bendall), Bios Scientific, Oxford, **1996**, pp. 43 – 68.
[2] a) L. Chen, R. C. Durley, B. J. Poliks, K. Hamada, Z. Chen, F. S. Mathews, V. L. Davidson, Y. Satow, E. Huizinga, F. M. Vellieux, *Biochemistry* **1992**, *31*, 4959 – 4964; b) H. Pelletier, J. Kraut, *Science* **1992**, *258*, 1748 – 1755; c) L. Chen, R. C. Durley, F. S. Mathews, V. L. Davidson, *Science* **1994**, *264*, 86 – 90; d) I. F. Sevrioukova, H. Li, H. Zhang, J. A. Peterson, T. Poulos, *Proc. Natl. Acad. Sci. USA* **1999**, *96*, 1863 – 1868; e) G. Kurisu, M. Kusunoki, E. Katoh, T. Yamazaki, K. Teshima, Y. Onda, Y. Kimata-Ariga, T. Hase, *Nat. Struct. Biol.* **2001**, *8*, 117 – 121; f) J. J. Müller, A. Lapko, G. Bourenkov, K. Ruckpaul, U. Heinemann, *J. Biol. Chem.* **2001**, *276*, 2786 – 2789.
[3] E. R. P. Zuiderweg, *Biochemistry* **2002**, *41*, 1 – 7.
[4] W. A. Cramer, G. M. Soriano, M. Ponamarev, D. Huang, H. Zhang, S. E. Martinez, J. L. Smith, *Annu. Rev. Plant Phys.* **1996**, *47*, 477 – 508.
[5] S. E. Martinez, D. Huang, A. Szczepaniak, W. A. Cramer, J. L. Smith, *Structure* **1994**, *2*, 95 – 105.
[6] C. J. Carrell, B. G. Schlarb, D. S. Bendall, C. J. Howe, W. A. Cramer, J. L. Smith, *Biochemistry* **1999**, *38*, 9590 – 9599.
[7] Y. I. Chi, L. S. Huang, Z. L. Zhang, J. G. Fernandez-Velasco, E. A. Berry, *Biochemistry* **2001**, *40*, 7689 – 7701.
[8] S. E. Martinez, D. Huang, M. Ponamarev, W. A. Cramer, J. L. Smith, *Protein Sci.* **1996**, *5*, 1081 – 1092.
[9] G. Sainz, C. J. Carrell, M. V. Ponamarev, G. M. Soriano, W. A. Cramer, J. L. Smith, *Biochemistry* **2000**, *39*, 9164 – 9173.
[10] C. S. Bond, D. S. Bendall, H. C. Freeman, J. M. Guss, C. J. Howe, M. J. Wagner, M. C. J. Wilce, *Acta Crytallogr. Sect. D* **1999**, *55*, 414 – 421.
[11] E. L. Gross in *Oxygenic Photosynthesis: The Light Reactions* (Eds.: D. R. Ort, C. F. Yocum), Kluwer Academic, Dordrecht, **1996**, pp. 413 – 429.
[12] K. Sigfridsson, *Photosynth. Res.* **1998**, *57*, 1 – 28.
[13] M. Ubbink, M. Ejdeback, B. G. Karlsson, D. S. Bendall, *Structure* **1998**, *6*, 323 – 335.
[14] P. B. Crowley, G. Otting, B. G. Schlarb-Ridley, G. W. Canters, M. Ubbink, *J. Am. Chem. Soc.* **2001**, *123*, 10444 – 10453.
[15] F. De Rienzo, R. R. Gabdoulline, M. C. Menziani, R. C. Wade, *Protein Sci.* **2000**, *9*, 1439 – 1454.
[16] M. Ubbink, D. S. Bendall, *Biochemistry* **1997**, *36*, 6326 – 6335.
[17] G. V. Louie, G. D. Brayer, *J. Mol. Biol.* **1990**, *214*, 527 – 555.
[18] A. Nicholls, K. Sharp, B. Honig, *Prot. Struc. Funct. Genet.* **1991**, *11*, 281 – 296.
[19] a) http://www.dq.fct.unl.pt/bioin/chemera/; b) P. N. Palma, L. Krippahl, J. E. Wampler, J. J. G. Moura, *Proteins* **2000**, *39*, 372 – 384.
[20] X. Morelli, A. Dolla, M. Czjzek, P. N. Palma, F. Blasco, L. Krippahl, J. J. G. Moura, F. Guerlesquin, *Biochemistry* **2000**, *39*, 2530 – 2537.
[21] P. N. Palma, I. Moura, J. Le Gall, J. van Beeumen, J. E. Wampler, J. J. G. Moura, *Biochemistry* **1994**, *33*, 6394 – 6407.
[22] M. R. Mauk, J. C. Ferrer, A. G. Mauk, *Biochemistry* **1994**, *33*, 12609 – 12614.
[23] R. M. Keller, K. Wütrich, *Biochim. Biophys. Acta.* **1978**, *553*, 195 – 208.
[24] A. J. Wand, D. L. Di Stefano, Y. Q. Feng, H. Roder, S. W. Englander, *Biochemistry* **1989**, *28*, 186 – 194.
[25] Y. Gao, J. Boyd, R. J. P. Williams, G. J. Pielak, *Biochemistry* **1990**, *29*, 6994 – 7003.
[26] S. E. J. Rigby, G. R. Moore, J. C. Gray, P. M. A. Gadsby, S. J. George, A. J. Thompson, *Biochem. J.* **1988**, 256, 571 – 577.
[27] P. J. Kraulis, *J. Appl. Crystallogr.* **1991**, *24*, 946 – 950.
[28] M. J. Wagner, J. C. L. Packer, C. J. Howe, D. S. Bendall, *BBA-Bioenergetics* **1996**, *1276*, 246 – 252.
[29] L. Lo Conte, C. Chothia, J. Janin, *J. Mol. Biol.* **1999**, *285*, 2177 – 2198.
[30] C. J. Carrell, H. Zhang, W. A. Cramer, J. L. Smith, *Structure* **1997**, *5*, 1613 – 1625.
[31] B. Schoepp, E. Chabaud, C. Breyton, A. Vermeglio, J. L. Popot, *J. Biol. Chem.* **2000**, *275*, 5275 – 5283.
[32] J. A. R. Worrall, U. Kolczak, G. W. Canters, M. Ubbink, *Biochemistry* **2001**, *40*, 7069 – 7076.
[33] G. M. Soriano, M. V. Ponamarev, R. A. Piskorowski, W. A. Cramer, *Biochemistry* **1998**, *37*, 15120 – 15128.
[34] L. Qin, N. M. Kostić, *Biochemistry* **1996**, *35*, 3379 – 3386.
[35] C. Frazao, C. M. Soares, M. A. Carrondo, E. Pohl, Z. Dauter, K. S. Wilson, M. Hervas, J. A. Navarro, M. A. De la Rosa, G. M. Sheldrick, *Structure* **1995**, *3*, 1159 – 1169.
[36] M. Hervas, J. A. Navarro, F. P. Molina-Heredia, M. A. De la Rosa, *Photosynth. Res.* **1998**, *57*, 93 – 100.
[37] W. B. R. Pollock, F. I. Rosell, M. B. Twitchett, M. E. Dumont, A. G. Mauk, *Biochemistry* **1998**, *37*, 6124 – 6131.
[38] A. S. Morar, D. Kakouras, G. B. Young, J. Boyd, G. J. Peilak, *J. Biol. Inorg. Chem.* **1999**, *4*, 220 – 222.
[39] B. G. Schlarb, M. J. Wagner, E. Vijgenboom, M. Ubbink, D. S. Bendall, C. J. Howe, *Gene* **1999**, *234*, 275 – 283.
[40] P. Andersson, B. Gsell, B. Wipf, H. Senn, G. Otting, *J. Biomol. NMR* **1998**, *11*, 279 – 288.
[41] C. Bartels, T.-H. Xia, M. Billeter, P. Güntert, K. Wüthrich, *J. Biomol. NMR* **1995**, *5*, 1 – 10.

Received: December 18, 2001 [F335]